Visualization and Characterization of Stability Swings via GPS-Synchronized Data

George J. Cokkinides, A. P. Sakis Meliopoulos, George Stefopoulos, Ramiz Alaileh and Apurva Mohan
School of Electrical and Computer Engineering
Georgia Institute of Technology
Atlanta, Georgia 30332 – 0250
Cokkinides@comcast.net

Abstract: *This paper provides a methodology to characterize the accuracy of PMU data (GPS-synchronized) and the applicability of this data for monitoring system stability via visualization methods. GPS-synchronized equipment (PMUs) is in general higher precision equipment as compared to typical SCADA systems. Conceptually, PMU data are time tagged with precision better than 1 microsecond and magnitude accuracy that is better than 0.1%. This potential performance is not achieved in an actual field installation due to errors from instrumentation channels and system imbalances. Presently, PMU data precision from substation installed devices is practically unknown. On the other hand, specific applications of PMU data require specific accuracy of data. Applications vary from simple system monitoring to wide area protection and control to voltage instability prediction and transient stability monitoring. The paper focuses on the last application, i.e. transient stability monitoring. We propose an approach that is based on accurate evaluation of the system energy function (Lyapunov indirect method) and extraction of stability properties from the energy function. Specifically, we provide a methodology for determining the required data accuracy for the reliable real time estimation of the energy function. When the data meet these requirements, the estimated energy function can be visualized and animated providing a powerful visual tool for observing the transient stability or instability of the system.*

***Index Terms*— PMU, GPS-synchronization, Data Accuracy, Energy Function, Transient Stability.**

Glossary
GPS: Global Positioning System
PMU: Phasor Measurement Unit
DSE: Dynamic State Estimation

Introduction

Monitoring the operating state of the system and assessing its stability in real time has been recognized as a task of paramount importance and a tool to avert blackouts. It is also recognized that when real time data are used to derive the real time dynamic model of the system, it is possible to predict the behavior of the system and therefore will enable preventive action. This paper presents preliminary work in this area. The paper is focused on the utilization of the available data for extracting a real time dynamic model which in turn is used to determine the stability of the system via energy functions. The described procedures are decentralized, i.e. the data are utilized at each substation/generating substation of the system and they are globally valid. It is shown that if GPS-synchronized data are available at each substation this is possible. We describe the technology of GPS-synchronized measurements first. The utilization of this data for extracting the real time dynamic model is described next. This model is used to predict system stability.

An important issue is the accuracy of the available data. Specifically, GPS-synchronized equipment (PMUs) is in general higher precision equipment as compared to typical SCADA systems. Conceptually, PMUs provide measurements that are time tagged with precision better than 1 microsecond and magnitude accuracy that is better than 0.1%. This potential performance is not achieved in an actual field installation because of two reasons: (a) different vendors use different design approaches that result in variable performance among vendors, for example use of multiplexing among channels or variable time latencies among manufacturers result in timing errors much greater than one microsecond, and (b) GPS-synchronized equipment receives inputs from instrument transformers, control cables, attenuators, etc. which introduce magnitude and phase errors that are much greater than the precision of PMUs. For example, many utilities may use CCVTs for instrument transformers. We refer to the errors introduced by instrument transformers, control cables, attenuators, etc. as the instrumentation channel error. The end result is that "raw" phasor data from different vendors cannot be used as highly accurate data.

GPS-synchronized data offer the possibility of dramatically improved applications, such as real time monitoring of the system, improved state estimation, direct state measurement, precise disturbance monitoring, transient instability prediction, wide area protection and control, voltage instability prediction and many others. For proper functioning of each one of these applications, a certain subset of data and a certain precision of data are required. Table 1 illustrates the data subset and precision required for different applications in a qualitative way. At this point the required data precision is categorized into (a) low, (b) moderate and (c) high. To quantify these descriptions is very difficult and depends on what performance can be accepted for each one of the listed applications.

1530-1605/07 $20.00 ©2007 IEEE

Table 1. Data Sets and Data Accuracy Requirements by Application

Application	Data Required	Required Data Accuracy
Steady State Monitoring	V, I	Low
Disturbance Monitoring	V, I, f	Moderate
State Measurement	V, I, f, df/dt	High
State Estimation	V, I	High
Wide Area Protection	V, I, f, df/dt	Moderate
Transient Instability Monitoring	V, I, f, df/dt	High

V: voltage, I: current, f: frequency, df/dt: rate of frequency change

Conceptually, the overall precision issue can be resolved with sophisticated calibration methods. This approach is quite expensive and faces difficult technical problems. Specifically, it is extremely difficult to calibrate instrument transformers and the overall instrumentation channel in the field. Laboratory calibration of instrument transformers is possible but a very expensive proposition if all instrument transformers need to be calibrated. In the early 90's the authors directed a research project in which we developed calibration procedures for selected NYPA's high voltage instrument transformers [9]. From the practical point of view, this approach is an economic impossibility. An alternative approach is to utilize appropriate filtering techniques for the purpose of correcting the magnitude and phase errors, assuming that the characteristics of the various GPS-synchronized equipment are known and the instrumentation feeding this equipment is also known.

We propose a viable and practical approach to correct for errors from instrumentation, system imbalances and data acquisition systems. Specifically, we have recently proposed the SuperCalibrator concept that consists of a filter (state estimation) of the voltage and current data using a three-phase, breaker oriented, instrumentation inclusive model. In this paper we extend this model to utilize the additional PMU data, namely frequency and rate of change of frequency, for extracting a real time dynamic model of the system. It is important to note that GPS synchronized measurements provide the frequency and rate of frequency change at the point of connection of the PMUs, typically the high voltage side of step-up transformers or the terminals of the generators. These measurements do not provide directly the speed of the generators (or motors) especially in cases where the impedance of the generator is comparable to the driving impedance of the network. This means that in order to extract an accurate dynamic model of the system, an appropriate estimation procedure must be applied. In this paper we propose a stability monitoring method that is integrated with the process of estimating the real time dynamic model of the system. The paper presents the two constituent parts of the overall approach: (a) the extension of the SuperCalibrator method to estimate the dynamic "state" of the system that includes generator speed and acceleration and (b) the utilization of the dynamic state of the system to extract stability or instability information using an energy function approach and visualizations and animations of the stability of the system. The proposed computational procedure may reside at the substation, and it can operate on the streaming data. The method can be implemented using standard communication protocols, such as the IEC 61850. The process is fast and therefore it can be applied on real time data on a continuous basis introducing only minor time latencies. The proposed methodology is based on a statistical estimation methodology that requires (a) the characteristics of GPS-synchronized equipment (PMUs), (b) a detailed model of the substation including the model of the instrumentation, and (c) the detailed model of generating units. Subsequent paragraphs present the models of the GPS-synchronized equipment as well as the substation and generating unit(s) model with the instrumentation channels.

Method Description

The methodology is based on a detailed, integrated model of the power system, instrumentation channel and data acquisition system. The power system model is a detailed three-phase, breaker oriented model and includes the substation, the generating units and the interconnected transmission lines. The instrumentation channel model includes instrument transformers, control cables, attenuators, burdens, and A/D converters. The modeling approach is physically based, i.e. each model is represented with the exact construction geometry and the electrical parameters are extracted with appropriate computational procedures. The model and system state include dynamics. The present work includes the dynamics of the generators represented with the speed and the acceleration of each generator. In the future we expect to augment the model with the load dynamics as well. As the data stream, each set of data at a specific time tag is processed via a general dynamic state estimation (DSE) process that "fits" the data to the integrated model. The overall approach is illustrated in Figure 1.

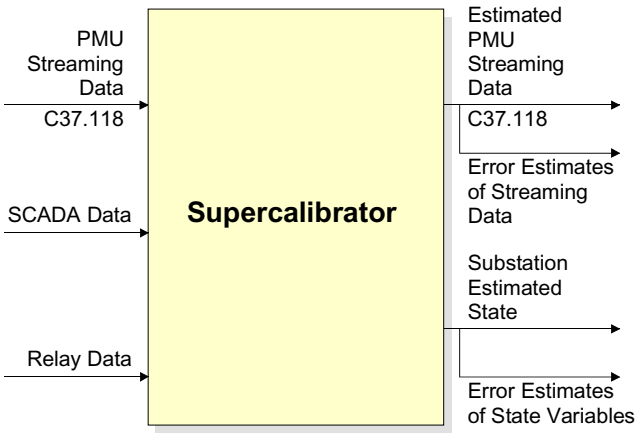

Figure 1. Inputs and Outputs of the SuperCalibrator

The procedure provides the best estimate of the data as well as performance metrics of the estimation process. The most important metric is the expected value of the error of the estimates. The best estimate of the data is used to regenerate the streaming data flow (this data is now filtered). Note that this model is an extension of our previous work on the SuperCalibrator approach. The new development here is the dynamic state estimator that can estimate the generating unit speed and acceleration from GPS-synchronized measurements.

Generating Substation State Estimation

The dynamic state estimator is typically applied to a generating substation. The objective is to extract the precise model of the generating system in real time, including the speed and acceleration of each generator. The model utilized in the estimation process is illustrated in the Appendix. Note that the form of the model is generically described as follows:

$$i = f_1(x, y, z)$$
$$0 = f_2(x, y, z)$$
$$0 = \frac{dz}{dt} + f_3(x, y, z)$$

where the functions f_1, f_2, f_3 are algebraic function of degree no greater than 2. Note that the model is a set of algebraic and differential equations. Obviously the differential equations express the dynamics of the system. In the present implementation we have included the dynamics of generators only. In future work the dynamics of the load will be included. The vector i are the terminal currents of the generator, x, y and z represent the state of the generator. The measurements in this system are: terminal voltages and currents (phasors), frequency and rate of frequency change. The model equations are given in Appendix A. A conceptual view of the system and measurements is illustrated in Figure 2. The state of the system is defined as the minimum number of independent variables that completely define the state of the system. For the substation of Figure 2 the state of the system consists of: (a) the phasor voltages of phases A, B and C of the two buses (transformer high side and low side), and (b) the generator speed (frequency) and acceleration (frequency rate of change). In summary, the state of the generating substation of Figure 2 is defined in terms of 6 complex variables and two real variables.

The number of measurements for this system from GPS-synchronized equipment, relays and standard SCADA system is quite large. Typically, the direct voltage measurements alone will have a redundancy of two to three, i.e. two to three times the number of voltage states. The available current measurements will generate a much larger redundancy considering that there will be CTs at each breaker, transformer, reactors, etc. For the system of Figure 2, and with a typical instrumentation, there will be more than 120 measurement data. This represents a redundancy level of 850%.

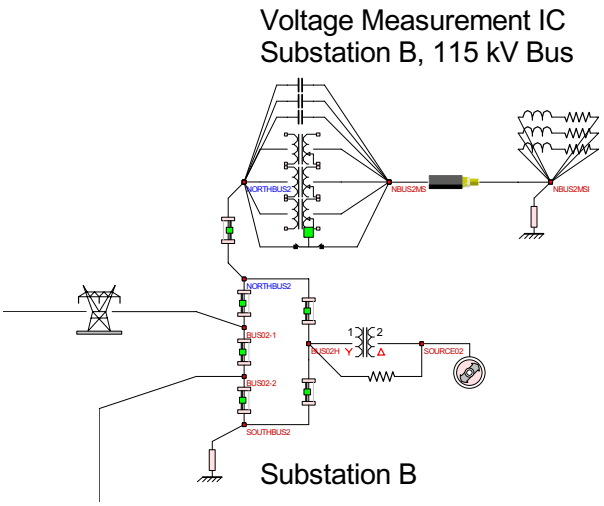

Figure 2. Breaker-Oriented Three-Phase Generating Substation Model

The state of the system, expressed with the variables x, y and z, is defined as the phasors of the phase voltages at each bus, the generator speed (frequency) and acceleration (rate of change of frequency) for each generating unit and a number of internal generator variables as described in Appendix A. A bus k will have three to five nodes, phases A, B and C, possibly a neutral and possibly a ground node. Under normal conditions the voltage at the neutral or ground will be very small and it will be assumed to be zero for this application. The state of the system at this bus is the node voltage phasors. We will use the following symbols:

The state vector x represents the voltage phasors:

$$\tilde{V}_{k,A} = \tilde{V}_{k,A} = V_{k,A,r} + jV_{k,A,i}$$
$$\tilde{V}_{k,B} = \tilde{V}_{k,B} = V_{k,B,r} + jV_{k,B,i}$$
$$\tilde{V}_{k,C} = \tilde{V}_{k,C} = V_{k,C,r} + jV_{k,C,i}$$

The state vector z represents the frequency (speed) and rate of frequency change (acceleration):

$$f_{gi}, and \frac{df_{gi}}{dt}$$

The state vector y represents internal state variables needed for the quadratization of the model. Note that while PMUs do measure the frequency and rate of frequency change at the location where they are connected, the measurements are not equal to the actual frequency (speed) and rate of frequency change (acceleration) at the generating unit.

The measurements can be GPS-synchronized measurements, relay data or usual SCADA data. A typical list of measurement data is given in Table 2. The measurements are

assumed to have an error that is statistically described with the meter accuracy.

Table 2. List of Measurements

Phasor Measurements Description	Non-synchronized Measurements Description
Voltage Phasor, $\tilde{V}$	Voltage Magnitude, V
Current Phasor, $\tilde{I}$	Real Power Flow, P_f
Current Inj. Phasor, $\tilde{I}_{inj}$	Reactive Power Flow, Q_f
Frequency	Real Power Injection, P_{inj}
Rate of frequency change	Reactive Power Inj., Q_{inj}

For monitoring the stability of the system it is imperative that the state of the generator is identified as accurately as possible. In this respect it is necessary to recognize that the instrumentation channel introduces substantial errors much higher than the errors introduced by the measuring device itself. It is also important to recognize that in a transient condition the frequency and the rate of frequency change will be different at different points of the system. For this reason the instrumentation channel model as well as the dynamic models of the generators (and other dynamic components) are included in the overall approach. Specifically, the instrumentation channel is modeled and each measurement is related to the state of the system via the transfer function of the instrumentation channel. We write:

GPS synchronized measurements:

$$z_{rj} + jz_{ij} = g_j(x, y, z), \text{ for measurement } j$$

Non-synchronized measurements:

$$z_k = g_k(x, y, z), \text{ for measurement } k$$

The model of the instrumentation channel and its gain function is obtained from the physical characteristics of the instrument transformers, control cable, termination impedances, A/D conversion devices, etc.

It is also important to recognize that it is not practical to measure the generator internal states. In this case it may appear that we do not have enough measurements to perform a state estimation. This is not true. We do have a number of equations that relate the internal generator states to other states. Each one of these equations can be viewed as a measurement with certainty. We refer to these as pseudomeasurements which are added to the measurement set. A partial list of pseudomeasurements is described in Appendix B.

Description of the Dynamic State Estimator (DSE)

Given a set of measurements, the state of the system is computed via the well known state estimation approaches. We elected to apply a least square approach to this problem as follows. First the differential equations are integrated with the quadratic method [1]. This procedure makes the system model a set of algebraic equations in which the dynamic states assume discrete values at specific time instances. We denote the algebraic equations with the state vector $h(x)$. Then a measurement z_i will be expressed as:

$$z_i = g_i(h_i(x))$$

The state is computed from the solution of the following optimization problem.

$$Min \quad J = \sum_i \left(\frac{z_i - g_i(h_i(x))}{\sigma_i} \right)^2$$

where σ_i is the meter accuracy.

Note that the above simple procedure has converted a dynamic estimation problem to a static state estimation problem. Solution methods for above problem are well known. In subsequent paragraphs, the models of the measurements and the details of the hybrid state estimator are described.

By manipulating the above equations, the measurements will have a general form as follows:

GPS-synchronized measurements:

$$z_s = H_s x + \eta_s$$

Non-synchronized measurements

$$z_n = H_n x + \{x^T Q_i x\} + \eta_n$$

The pseudomeasurements are in general quadratic equations, similar to above equations (in form).

Now, the state estimation problem is formulated as follows:

$$Min \quad J = \sum_{v \in phasor} \frac{\tilde{\eta}_v^* \tilde{\eta}_v}{\sigma_v^2} + \sum_{v \in non-syn} \frac{\eta_v \eta_v}{\sigma_v^2}$$

Using the above quadratic formulation and the separation of the measurements into phasor, non-synchronized and pseudomeasurements as has been indicated earlier, the general form of the measurements is:

$z_s = H_s x + \eta_s$, GPS-synchronized measurements

$z_n = H_n x + \{x^T Q_i x\} + \eta_n$, non-synchronized

$z_p = 0 = H_p x + \{x^T Q_i x\} + \eta_p$, pseudomeasurements

In above equations, the subscript s indicates phasor measurements, the subscript n indicates non-synchronized measurements and the subscript p indicates pseudomeasurements. The best state estimate is given by:

Case 1: Phasor measurements only.

$$\hat{x} = \left(H_s^T W H_s\right)^{-1} H_s^T W z_s$$

Case 2: Phasor, non-synchronized and pseudomeasurements.

$$\hat{x}^{\nu+1} = \hat{x}^{\nu} + \left(H^T W H\right)^{-1} H^T W \begin{bmatrix} z_s - H_s \hat{x}^{\nu} \\ z_n - H_n \hat{x}^{\nu} - \left\{\hat{x}^{\nu T} Q_i \hat{x}^{\nu}\right\} \end{bmatrix}$$

where:

$$W = \begin{bmatrix} W_s & 0 \\ 0 & W_n \end{bmatrix}, \qquad H = \begin{bmatrix} H_s \\ H_n + H_{qn} \end{bmatrix}$$

Implementation

The proposed methodology for correcting errors from various manufacturers is being implemented into a general state estimation method. The computer model has been named the SuperCalibrator. Presently the methodology operates on the data from one substation at a time. The overall approach is shown in Figure 3. The data are collected from each IED and are sorted by time tag into sets of data taken at exactly the same time instant. Presently this process is done in a semi-automated way. Specifically, the data from each IED is collected in a COMTRADE format and processed into providing data sets in time instances, t1, t2, etc. In the future this process will be fully automated. The substation PDC shown in Figure 3 is a personal computer that collects the data and runs the SuperCalibrator with the Dynamic State Estimator. The end result is the real time dynamic state of the system. This model is subsequently utilized to characterize the stability of the system and to provide visualizations of the stability condition of the system.

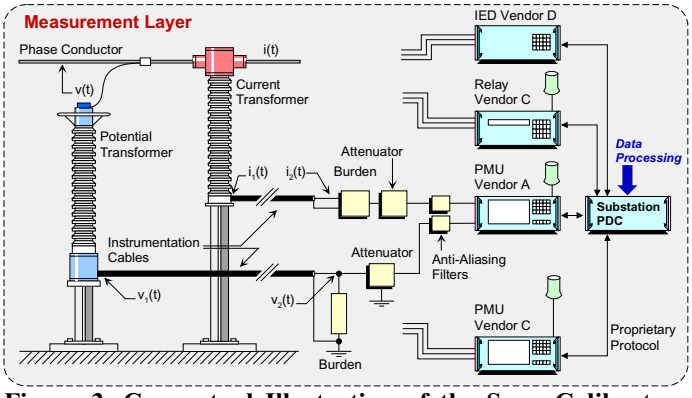

Figure 3. Conceptual Illustration of the SuperCalibrator with Dynamic State Estimator

Application to Stability Monitoring

The real time dynamic state of the substation that includes the full operating condition of the generators is utilized to characterize and predict the stability of the system. Specifically this model contains the generator speed, torque angle and acceleration. This information is enough to monitor the dynamics of the generator. Use of visualization techniques can display this information in a meaningful way to system operators. As an example, Figure 4 illustrates such visualization. Note that the visualization shows many generators as it will be the case when the SuperCalibrator is implemented in all generating substations. The visualization shows the position of each generator according to its torque angle. In addition the speed of the generator (above or below synchronous speed) is shown with arrows that are proportional to the numerical value of the speed. Note that as the information is updated from the SuperCalibrator, the visualization provides an animation of the motion of the system. Specifically, the SuperCalibrator may "run" at a rate of 60 times per second thus updating the visualization 60 times a second. This refresh speed is more than adequate to provide an excellent animation of the dynamics of the system in real time. The animation indirectly provides a feel of the acceleration of the generating units as their position and/or the arrow size of the speed changes. This visualization will be demonstrated at the presentation of the paper.

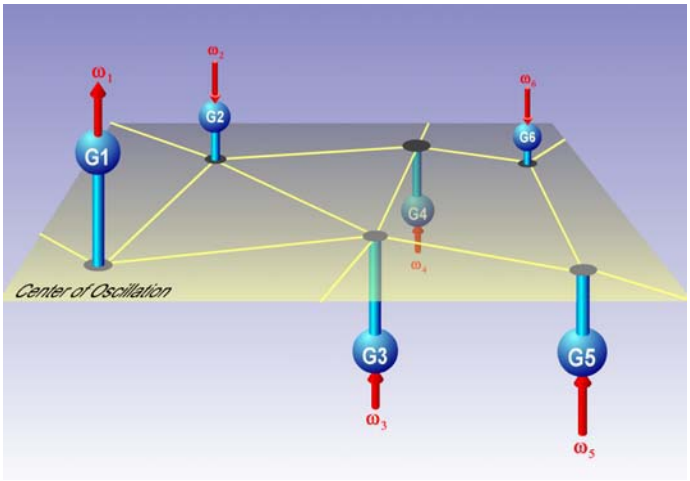

Figure 4. Visualization of Generator Real Time State

We also propose to go one step further. Specifically, we propose to use this information to predict the stability of the system. For this purpose we use the output of the real time dynamic model of the system to compute the total energy of the system. Note that the total energy of the system is defined in terms of generator torque angle and speed. Using the quadratic formulation of this paper the energy function is also a quadratic equation of the form (defined in the usual way of the sum of the potential energy plus the kinetic energy):

$$V(x(t)) = P_1^T x_N + x_N^T(t) P_2 x_N(t)$$

Note that this form includes the state variables c and s see appendix which are transcendental equations (sines and cosines). They define the stability region in the usual way via the separatrix. Having this function a number of visualizations are implemented. For example Figure 5 illustrates the operating condition of the generator as a blue dot superimposed on a 2-D visualization of the potential energy function. Figure 5a visualizes a generator that has a total energy that is less than the maximum potential energy (lower than the barrier at the separatrix. This system is stable and therefore the oscillations eventually will decay and the system will return to steady state operating conditions. Figure 5b provides a visualization of a generator that has total energy above the potential energy at the barrier (separatrix). This system is unstable and the oscillations will lead to system separation. Figure 6 provides another visualization of the generator oscillations. Specifically it illustrates the motion of the unit in a speed versus rotor position 2-D visualization superimposed on the graph of the separatrix on the same 2-D visualization. If the motion of the unit comes closer to the separatrix without crossing it indicates an oscillatory but stable swing. If it crosses the separatrix in indicates an unstable swing. The separatrix is computed from the energy function. Finally, Figure 7 illustrates a 3-D visualization of the potential energy function. These visualizations are useful not only to provide the stability swing of the system but also to predict whether the swing is stable or unstable. Note that the visualizations of Figures 5a and 5b provide the capability to predict the instability with some advance time (typically up to half second depending on the parameters of the system). This is very useful for relaying applications since human respond cannot be that fast.

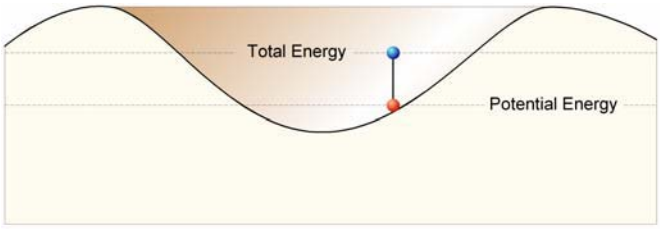

Figure 5a. 2-D Visualization of Generator Operating Point and Potential Energy – Stable Oscillation

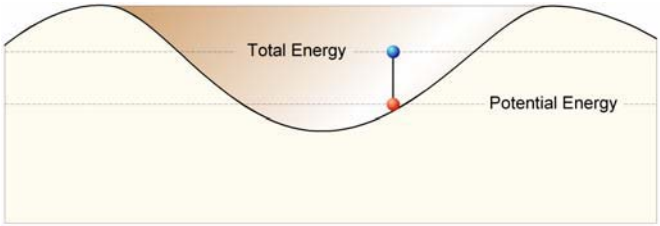

Figure 5b. 2-D Visualization of Generator Operating Point and Potential Energy – Unstable Oscillation

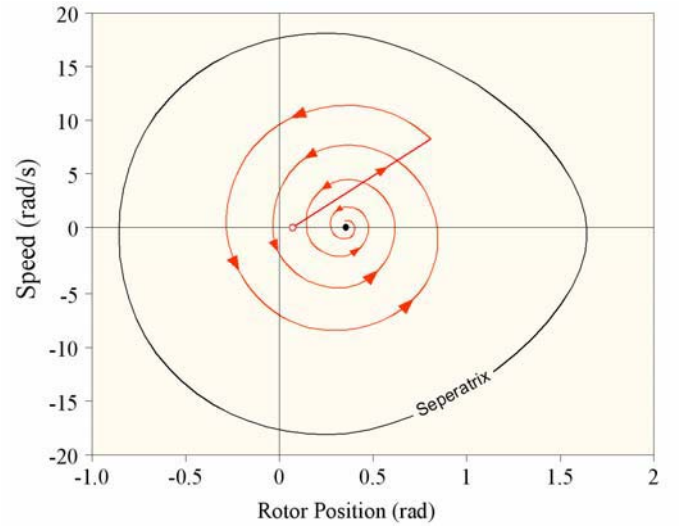

Figure 6. 2-D Visualization of Generator Trajectory in a Speed-Rotor Position Plane with Separatrix

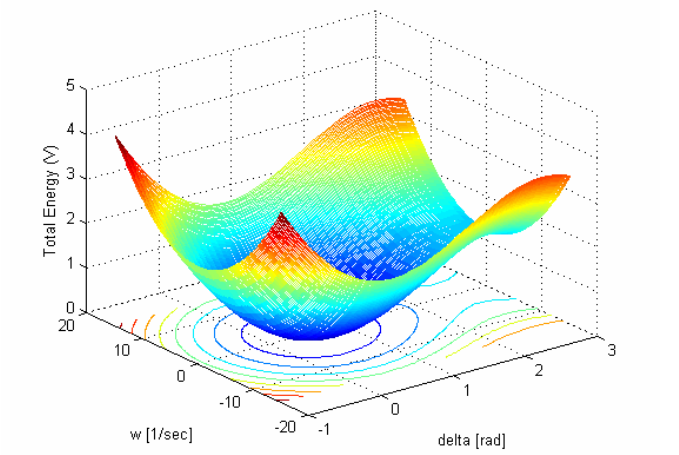

Figure 7. 3-D Visualization of Generator Energy Function

Conclusions

This paper presented methodologies for filtering available data in substations (for example phasor data, relay data and SCADA data) for the purpose of extracting a real time dynamical model of the system. The real time dynamical model is used for monitoring system stability and it is capable to predict any instability that may arise.

The innovations presented here is (a) the extension of the SuperCalibrator to perform dynamic state estimation (DSE) and (b) the entire filtering process (DSE) is confined to the substation, using a three-phase, breaker oriented, instrumentation inclusive and generator dynamics inclusive substation model. The methodology provides the means for correcting errors from instrumentation channels, phase shifts of different PMU manufacturers and accommodates unbalanced operation and system model asymmetries.

The proposed extension of the SuperCalibrator provides a precise dynamic state estimator for power systems at the substation level. The estimator is ideally suited for monitoring the stability of the system as well as predicting any instability before it occurs. Applications of these concepts can be extended to protection of the system with improved out of step protection and wide area special protection schemes.

Future work will focus on including the electric load dynamics in the model for the purpose of assessing the effects of load dynamics in system stability.

Acknowledgments

The work reported in this paper has been partially supported by the NSF Grant No. 000812, PSERC project S-25 and by the CTC project. This support is gratefully acknowledged.

References

1. A. P. Meliopoulos, G. J. Cokkinides, George K. Stefopoulos, "Quadratic Integration Method", *Proceedings of the 2005 International Power System Transients Conference (IPST 2005)*, p. xx (pp. x-x), Montreal, Canada, June 19-23, 2005.
2. A. P. Sakis Meliopoulos and G. J. Cokkinides, "Visualization and Animation of Instrumentation Channel Effects on DFR Data Accuracy", Proceedings of the 2002 Georgia Tech Fault and Disturbance Analysis Conference, Atlanta, Georgia, April 29-30, 2002
3. T. K. Hamrita, B. S. Heck and A. P. Sakis Meliopoulos, 'On-Line Correction of Errors Introduced By Instrument Transformers In Transmission-Level Power Waveform Steady-State Measurements', *IEEE Transactions on Power Delivery*, Vol. 15, No. 4, pp 1116-1120, October 2000.
4. A. P. Sakis Meliopoulos and George J. Cokkinides, "Virtual Power System Laboratories: Is the Technology Ready?", *Proceedings of the 2000 IEEE/PES Summer Meeting*, Seattle, WA, July 16-20, 2000.
5. A. P. Sakis Meliopoulos and George J. Cokkinides, 'A Virtual Environment for Protective Relaying Evaluation and Testing', *Proceedings of the 34st Annual Hawaii International Conference on System Sciences*, p. 44 (pp. 1-6), Wailea, Maui, Hawaii, January 3-6, 2001.
6. A. P. Sakis Meliopoulos, George J. Cokkinides, "Visualization and Animation of Protective Relays Operation From DFR Data", *Proceedings of the 2001 Georgia Tech Fault and Disturbance Analysis Conference*, Atlanta, Georgia, April 30-May 1, 2001.
7. A. P. Meliopoulos and J. F. Masson, "Modeling and Analysis of URD Cable Systems," *IEEE Transactions on Power Delivery*, vol. PWRD-5, no. 2, pp. 806-815, April 1990.
8. G. P. Christoforidis and A. P. Sakis Meliopoulos, "Effects of Modeling on the Accuracy of Harmonic Analysis," *IEEE Transactions on Power Delivery*, vol. 5, no. 3, pp.1598-1607, July 1990.
9. A. P. Meliopoulos, F. Zhang, S. Zelingher, G. Stillmam, G. J. Cokkinides, L. Coffeen, R. Burnett, J. McBride, 'Transmission Level Instrument Transformers and Transient Event Recorders Characterization for Harmonic Measurements,' *IEEE Transactions on Power Delivery*, Vol 8, No. 3, pp 1507-1517, July 1993.
10. B. Fardanesh, S. Zelingher, A. P. Sakis Meliopoulos, G. Cokkinides and Jim Ingleson, 'Multifunctional Synchronized Measurement Network', *IEEE Computer Applications in Power*, Volume 11, Number 1, pp 26-30, January 1998.
11. A. P. Sakis Meliopoulos and G. J. Cokkinides, "Phasor Data Accuracy Enhancement in a Multi-Vendor Environment", Proceedings of the 2005 Georgia Tech Fault and Disturbance Analysis Conference, Atlanta, Georgia, April 25-26, 2005
12. F. Darema, "Dynamic Data Driven Application Systems," Presentation at Purdue University, May 4, 2004, http://www.cise.nsf.gov/eia/dddas
13. L. Tsoukalas, R. Gao, T. Fieno, X. Wang, "Anticipatory Regulation of Complex Power Systems," *Proc. of European Workshop on Intelligent Forecasting, Diagnosis and Control- IFDICON 2001*, Santorini, Greece, June 2001
14. A.P. Sakis Meliopoulos and George J. Cokkinides, "A Virtual Environment for Protective Relaying Evaluation and Testing", *IEEE Transactions of Power Systems*, Vol. 19, No. 1, pp. 104-111, February, 2004.

Biographies

George Cokkinides (M '85) was born in Athens, Greece, in 1955. He obtained the B.S., M.S., and Ph.D. degrees at the Georgia Institute of Technology in 1978, 1980, and 1985, respectively. From 1983 to 1985, he was a research engineer at the Georgia Tech Research Institute. Since 1985, he has been with the University of South Carolina where he is presently an Associate Professor of Electrical Engineering. His research interests include power system modeling and simulation, power electronics applications, power system harmonics, and measurement instrumentation. Dr. Cokkinides is a member of the IEEE/PES.

Sakis Meliopoulos (M '76, SM '83, F '93) was born in Katerini, Greece, in 1949. He received the M.E. and E.E. diploma from the National Technical University of Athens, Greece, in 1972; the M.S.E.E. and Ph.D. degrees from the Georgia Institute of Technology in 1974 and 1976, respectively. In 1971, he worked for Western Electric in Atlanta, Georgia. In 1976, he joined the Faculty of Electrical Engineering, Georgia Institute of Technology, where he is presently a professor. He is active in teaching and research in the general areas of modeling, analysis, and control of power systems. He has made significant contributions to power system grounding, harmonics, and reliability assessment of power systems. He is the author of the books, *Power Systems Grounding and Transients*, Marcel Dekker, June 1988, *Ligthning and Overvoltage Protection*, Section 27, Standard Handbook for Electrical Engineers, McGraw Hill, 1993, and the monograph, *Numerical Solution Methods of Algebraic Equations*, EPRI monograph series. Dr. Meliopoulos is a member of the Hellenic Society of Professional Engineering and the Sigma Xi.

George K. Stefopoulos (S '98) was born in Athens, Greece in 1977. He received the Diploma in Electrical and Computer Engineering from the National Technical University of Athens, Greece, in 2001 and the M.S. degree in E.C.E. from the Georgia Institute of Technology, Atlanta, GA, U.S.A., in 2002. He is currently a Ph.D. student at the School of Electrical and Computer Engineering of Georgia Institute of Technology. He is a student member of IEEE, IET, HKN (Eta Kappa Nu) and a member of the Technical Chamber of Greece.

Ramiz H. Alaileh (S '99) was born in Dubai, UAE in 1980. He received the B.Sc. in electrical engineering from the American University of Sharjah, UAE, in 2002 and the M.S. degree in electrical and computer engineering from the Georgia Institute of Technology in 2005. From 2003 to 2004, he has been with the Dubai Electricity and Water Authority (DEWA), UAE, as an energy management systems (EMS) engineer. He is currently a Ph.D. student at the School of Electrical and Computer Engineering of the Georgia Institute of Technology. He is a student member of IEEE. His research interests include power system stability, energy management systems, and power system protection.

Appendix A: Quadratized Two-Axes Generator Model

A two-axis quadratized synchronous generator model is presented here. The phasor diagram is presented in Figure A-1. The rotor position (d-axis) $\theta(t)$ as a function of rotor angular velocity $\omega(t)$ is:

$$\delta(t) = \theta(t) - \omega_s t - \frac{\pi}{2}, \qquad)$$

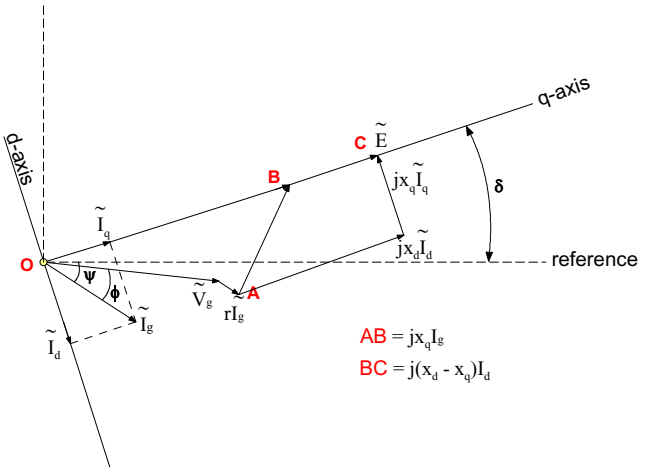

Figure A-1. Two-axis synchronous machine phasor diagram

The quadratized model is (it is equivalent to the standard two axes model – no simplifications):

$$\tilde{I}_g = \tilde{I}_d + \tilde{I}_q$$
$$0 = \tilde{E} - \tilde{V}_g + r(\tilde{I}_d + \tilde{I}_q) + jx_d\tilde{I}_d + jx_q\tilde{I}_q$$
$$0 = E_r I_{dr} + E_i I_{di}$$
$$0 = E_r s(t) - E_i c(t)$$
$$0 = E_i I_{qr} - E_r I_{qi}$$
$$0 = E_r^2 + E_i^2 - E_{spec.}$$
$$0 = T_a(t) - T_m(t) + 3\cdot z_1\left(I_{dr} + I_{qr}\right) + 3\cdot z_2\left(I_{di} + I_{qi}\right) + D\cdot\left(\omega(t) - \omega_s\right)$$
$$0 = z_1\omega(t) - E_r$$
$$0 = z_2\omega(t) - E_i$$
$$0 = w_1(t) - c(t)\cdot\omega(t) + \omega_s c(t)$$
$$0 = w_2(t) + s(t)\cdot\omega(t) - \omega_s s(t)$$
$$\frac{d\delta(t)}{dt} = \omega(t) - \omega_s$$
$$\frac{d\omega(t)}{dt} = \frac{\omega_s}{2H}T_a(t)$$
$$\frac{ds(t)}{dt} = w_1(t)$$
$$\frac{dc(t)}{dt} = w_2(t)$$

where

$\tilde{I}_g$: armature current (positive direction is into the generator),
r : armature resistance,
x_d : direct-axis synchronous reactance,
x_q : quadrature-axis synchronous reactance,
$\tilde{V}_g$: terminal voltage,
ω_s : synchronous speed,
H : inertia constant of the generator,
T_m : mechanical power supplied by a prime-mover (in p.u.),
T_D : damping torque (p.u.), which can be approximated by $T_D = D\cdot(\omega - \omega_s)$ with D constant,
$\tilde{E} = Ee^{j\delta}$ is the internal generator voltage; it is an input to the model and its magnitude is specified by an exciter system.

The state vector of the model is defined as:

$x^T = \left[x_1^T\, x_2^T\right]$,

with

$x_1^T = \left[\tilde{V}_g \quad \tilde{E} \quad \tilde{I}_d \quad \tilde{I}_q\right]$,

$x_2^T = \left[T_a(t) \quad z_1(t) \quad z_2(t) \quad w_1(t) \quad w_2(t) \quad \delta(t) \quad \omega(t) \quad s(t) \quad c(t)\right]$.

Appendix B: Pseudomeasurements for Generator Internal States

Since it is not practical to measure the generator internal states including additional variables introduced by the quadratization, a number of pseudomeasurements are introduced that provide the generator internal states and the additional variables. The introduction of the pseudomeasurements is a very simple procedure. First for the cos and sin variables, we perform the following computation:

The vector A below defines the q-axis (see geometric construction in Figure A-1):

$$\tilde{A} = \tilde{V}_g + r\tilde{I}_a + jx_q\tilde{I}_a$$

This computation provides the angle $\delta(t)$ and the variables $c(t) = \cos(\delta(t)), \; and \; s(t) = \sin(\delta(t))$. The computed values are treated as measurements with very small uncertainty. In addition each of the algebraic internal equations is also treated as a measurement with very small uncertainty. As an example consider the fifth equation of the model. This equation is treated as a measurement z, with measured value of zero and standard deviation a very small number epsilon, i.e.

$$z = 0 = E_i I_{qr} - E_r I_{qi} + \eta, \quad Var(\eta) = \varepsilon^2$$